NERC Open Research Archive sharing our research

Centre for Ecology & Hydrology
NATURAL ENVIRONMENT RESEARCH COUNCIL

Article (refereed)

Slater, Frances R.; **Singer, Andrew C.**; Turner, Susan; Barr, Jeremy J.; Bond, Philip L.. 2011 Pandemic pharmaceutical dosing effects on wastewater treatment: no adaptation of activated sludge bacteria to degrade the antiviral drug Oseltamivir (Tamiflu) and loss of nutrient removal performance. *FEMS Microbiology Letters*, 315 (1). 17-22. 10.1111/j.1574-6968.2010.02163.x

This version available http://nora.nerc.ac.uk/12274/

NERC has developed NORA to enable users to access research outputs wholly or partially funded by NERC. Copyright and other rights for material on this site are retained by the authors and/or other rights owners. Users should read the terms and conditions of use of this material at http://nora.nerc.ac.uk/policies.html#access

This document is the author's final manuscript version of the journal article, incorporating any revisions agreed during the peer review process. Some differences between this and the publisher's version remain. You are advised to consult the publisher's version if you wish to cite from this article.

The definitive version is available at www.interscience.wiley.com

Contact CEH NORA team at
noraceh@ceh.ac.uk

The NERC and CEH trade marks and logos ('the Trademarks') are registered trademarks of NERC in the UK and other countries, and may not be used without the prior written consent of the Trademark owner.

Pandemic pharmaceutical dosing effects on wastewater treatment: no adaptation of activated sludge bacteria to degrade the antiviral drug Oseltamivir (Tamiflu) and loss of nutrient removal performance

Slater, F.R.[1], Singer, A.C.[2], Turner, S.[3], Barr, J.J.[1] & Bond, P.L. [1*]

For submission to FEMS Microbiology Letters

[1] The University of Queensland, Advanced Water Management Centre (AWMC), Australia.

[2]The Centre for Ecology and Hydrology, Wallingford, United Kingdom.

[3]The University of Auckland, New Zealand.

*__Corresponding author__. Mailing address: Advanced Water Management Centre (AWMC), The University of Queensland, Level 6, Gehrmann Laboratories, Research Road, St. Lucia, QLD 4072. Telephone: +61 7 334 63226. Fax: +61 7 336 54726 E-mail: phil.bond@awmc.uq.edu.au

Keywords:

Antiviral degradation, pharmaceutical ecotoxicity, enhanced biological phosphorus removal (EBPR)

Running title: Pandemic pharmaceutical dosing effects on activated sludge

This is an Accepted Article that has been peer-reviewed and approved for publication in the *FEMS Microbiology Letters*, but has yet to undergo copy-editing and proof correction. Please cite this article as an "Accepted Article"; doi: 10.1111/j.1574-6968.2010.02163.x

ABSTRACT

The 2009-2010 influenza pandemic saw many people treated with antivirals and antibiotics. High proportions of both classes of drugs are excreted and enter wastewater treatment plants (WWTPs) in biologically active forms. To date, there has been no study into the potential for influenza pandemic-scale pharmaceutical use to disrupt WWTP function. Furthermore, there is currently little indication as to whether WWTP microbial consortia can degrade antiviral neuraminidase inhibitors when exposed to pandemic-scale doses. In this study, we exposed an aerobic granular sludge sequencing batch reactor, operated for enhanced biological phosphorus removal (EBPR), to a simulated influenza-pandemic dosing of antibiotics and antivirals for 8 weeks. We monitored removal of the active form of Tamiflu, oseltamivir carboxylate (OC), bacterial community structure, granule structure and changes in EBPR and nitrification performance. There was little removal of OC by sludge and no evidence that the activated sludge community adapted to degrade OC. There was evidence of changes to bacterial community structure and disruption to EBPR and nitrification during and after high-OC dosing. This work highlights the potential for antiviral contamination of receiving waters and indicates the risk of destabilising WWTP microbial consortia as a result of high concentrations of bioactive pharmaceuticals during an influenza pandemic.

INTRODUCTION

Society has never been more prepared for the emergence of pandemic influenza than at present, due in part to the development and stockpiling of a novel class of antiviral drugs, neuraminidase inhibitors, notably: Tamiflu® (oseltamivir ethylester-phosphate (OP)) and Relenza® (zanamivir). National stockpiling of neuramindase inhibitors began in earnest with the emergence of the 2009 influenza pandemic (H1N1). These stockpiles were dominated by Tamiflu largely owing to its relative ease of administration (tablet), as compared with Relenza (disc-inhaler). Tamiflu is a prodrug which, after absorption into the blood, is converted to the active antiviral, oseltamivir carboxylate (OC) in the liver. Approximately 80% of an oral dose of Tamiflu is excreted as OC in the urine (He et al., 1999), with the remainder excreted as OP in the faeces. Both the parent chemical and its bioactive metabolite ultimately reach the receiving wastewater treatment plants (WWTPs) where it was projected to reach a mean of ~2 to 12 μg L^{-1} during a moderate and severe pandemic respectively (Singer et al., submitted).

Current evidence suggests conservation of OC as it passes through WWTPs (Accinelli et al., 2010, Fick et al., 2007, Ghosh et al., 2010, Prasse et al., Soderstrom et al., 2010), hence, rivers receiving WWTP effluent will also be exposed to OC throughout a pandemic. Concentrations of between 293 and 480 ng OC L^{-1} have been recorded in rivers receiving WWTP effluent during the 2009 pandemic (Ghosh et al., 2010, Soderstrom et al., 2010). Several studies have demonstrated the potential for removal of OC from fresh water (amended in some cases with sediment) and activated sludge (amended in some cases with a granular bioplastic formulation entrapping propagules of white rot fungi) via adsorption, microbial degradation and indirect photolysis (Accinelli et al., 2007, Accinelli et al., 2010, Bartels and von Tumpling, 2008, Sacca et al., 2009). A key factor in determining the amount of OC removal appears to be the length of incubation, with batch incubations of 40 days

68 resulting in degradation of up to 76% OC in the presence of an activated sludge inoculum
69 (Accinelli et al., 2010). However, batch experiments do not reflect the activities of a WWTP
70 as the hydraulic residence time for wastewater in the activated sludge system is commonly
71 only a few hours and degradation would therefore be expected to be much lower. In a
72 pandemic scenario, Tamiflu use would rapidly rise over an 8 week period as the outbreak
73 spread and would follow a similarly rapid decline after the peak (Singer et al., 2007, Singer et
74 al., 2008, Singer et al., submitted). We hypothesise that the prolonged exposure of WWTP
75 microbial consortia over the course of a pandemic might hasten the generation of OC-
76 degraders in the activated sludge bacterial community thereby minimising the risks posed
77 from widespread environmental release.
78 The key processes in WWTPs (removal of organic carbon, nitrogen (N) and phosphorus (P)),
79 are microbiologically mediated by activated sludge. Activated sludge systems are constantly
80 exposed to pharmaceuticals from a variety of sources (Daughton and Ternes, 1999), however,
81 it remains unclear as to their effective toxicity (i.e., impact on nutrient removal performance).
82 The functioning of activated sludge under a pandemic scenario is of concern given the
83 projected heavy usage of not only antivirals but also antibiotics (ABs) (Singer et al., 2008,
84 Singer et al., submitted). There is recent evidence that bacterial neuraminidases are important
85 in biofilm formation (Parker et al., 2009, Soong et al., 2006). Consequently, antiviral
86 neuramindase inhibitors themselves may inhibit bacterial neuraminidases which could prove
87 detrimental to the structure of the suspended biofilms that make up activated sludge. Whilst
88 this is yet to be fully investigated, current data indicate that the ecotoxicological risks posed
89 by OC are low (Straub, 2009).
90 In addition to examining the potential evolution of OC-degradation in a microbial consortium
91 we aimed to investigate the effects of OC and ABs on activated sludge bacterial community
92 structure and function and activated sludge biofilm structure. We implemented a 56-day,

93 pandemic-scenario dosing regime of OC and three ABs (with different modes of action):
94 amoxicillin (cell-wall-synthesis inhibition), erythromycin (protein-synthesis inhibition) and
95 levofloxacin (DNA-replication inhibition), in a laboratory-scale sequencing batch reactor
96 (SBR) operated for granular enhanced biological phosphorus removal (EBPR). The three
97 antibiotics selected for this study are among the most frequently employed antibiotics, within
98 their class, for the treatment of influenza-associated bacterial pneumonia (Lim et al., 2007).
99 An additional high OC dosing period without ABs was employed to examine OC toxicity and
100 WWTP function in the absence of the presumed AB stress.
101
102

MATERIALS AND METHODS

Reactor Operation

A laboratory-scale sequencing batch reactor (SBR) had a working volume of 8 L, with 2 L of treated wastewater removed and replaced with synthetic influent wastewater every 6 h, resulting in a hydraulic retention time (HRT) of 24 h. The sludge age was approximately 24 days. The synthetic influent wastewater contained either acetate or propionate as the sole carbon source (alternated on a fortnightly basis; Lu et al., 2006) and orthophosphate ($P\text{-}PO_4^{3-}$) at concentrations of approximately 1100 mg chemical oxygen demand (COD) L^{-1} and 23 mg $P\text{-}PO_4^{3-}$ L^{-1} respectively (see SI for further details). The SBR was operated for EBPR, an activated sludge process for removing phosphate from wastewater. It is appropriate to investigate because it is commonly used in full-scale WWTPs and the bacterial community and biochemical transformations involved are well characterised (Seviour et al., 2003). The current study used granular activated sludge as the reactor biomass. This is a novel activated sludge technology which selects for aggregates (>200 μm) which are larger than those occurring in conventional floccular activated sludge (de Kreuk et al., 2007).

The operational parameters necessary for EBPR include introducing the wastewater into an anaerobic phase of operation, with an aerobic phase following. Typically, during the anaerobic stage the carbon source is taken up and phosphate is released by the bacteria, then in the subsequent aerobic phase the phosphate is taken up by the bacteria, over and above that which was released in the anaerobic phase (Seviour et al., 2003). Prior to dosing of pharmaceuticals the SBR was performing good EBPR for more than 6 months. During dosing, the reactor operation did not change, except that the principal carbon source in the reactor feed was no longer alternated between acetate and propionate but rather only acetate was used in order to reduce the number of variables. OC and ABs were added as detailed below.

OC and AB dosing

The OC and AB dosing for the SBR mirrored projected usage in the United Kingdom, as per Singer et al. (submitted), with stepwise dosing up to the pandemic peak. OC and ABs were dissolved in sterile distilled water and added to autoclaved acetate feed. The maximum amount of each AB and OC in the reactor influent was: 36 µg L^{-1} OC, 70 µg L^{-1} amoxicillin, 30 µg L^{-1} erythromycin, and 10 µg L^{-1} levofloxacin. During the 14-day OC-only dosing period the reactor influent contained 360 µg OC L^{-1} (see Table S1). At the peak of the simulated pandemic the concentration of ABs and OC were ~2 to 20 × projected mean concentrations in WWTPs as per Singer et al. (submitted), during a moderate pandemic (R_0 = 2.3, where R_0 indicates the average number of infections generated by an infectious individual in a fully susceptible population) with conservative estimates of Tamiflu use within the populations, (30% of infected people utilise OC). Although the experimental concentration of pharmaceuticals in the reactor were above mean projected levels (Singer et al., submitted), they reflect a realistic worst-case scenario.

Measurement of OC

OC was quantified from the influent and effluent during a single cycle of the SBR on the final day of each dosing regime. Approximately 10 mL of each sample was filtered through a 0.22 µm disposable filter (Millipore, Billerica, MA, USA) into glass GC vials and kept at -20 ^{o}C until measurement. OC concentrations were measured by direct aqueous injection of the sample into an Agilent 6410B Triple Quad LC MS at the National Laboratory Services (Wales) (see SI for further details).

Biochemical analyses

Mixed liquor suspended solids (MLSS), effluent suspended solids (effluent SS) and mixed liquor volatile suspended solids (VSS) were measured according to standard methods (APHA, 1998). Ammonium ($N\text{-}NH_4^+$), nitrate ($N\text{-}NO_3^-$), nitrite ($N\text{-}NO_2^-$), orthophosphate

($P\text{-}PO_4^{3-}$) and acetate concentrations in the liquid phase were analysed at the AWMC Analytical Laboratory (Brisbane, QLD, Australia) (see SI for further details).

Granule structure analyses

Visual inspections of whole granules were performed using an Olympus SZH10 stereo-microscope with a DP70 digital camera. Approximately 25 mL of mixed liquor was removed from the SBR at the end of the aerobic phase and photographed in a glass petri dish against a black background. Volumetric size distribution of granules was determined by pumping approximately 30 mL of mixed liquor (again, removed at the end of the aerobic phase) through a Malvern laser light scattering instrument (Mastersizer 2000 series, Malvern 457 Instruments, Worcestershire, UK).

T-RFLP

T-RFLP analysis of 16S rRNA genes was carried out as previously described (Slater et al., 2010) (see SI for further details).

Fluorescence *in situ* hybridisation (FISH)

Biomass samples were taken during the aerobic phase of the SBR and fixed in 4% paraformaldehyde in phosphate-buffered saline at $4^{o}C$ for 2 h. FISH was performed as described previously (Amann, 1995) (see SI for further details).

RESULTS

OC degradation

Over the experimental period there was evidence of varying rates of removal of OC (Figure 1). These were equivalent to between 2 and 41% removal per 6 h SBR cycle (estimated for each dosing period based on measured influent OC concentrations, four draw and fill cycles per day (Figure S1), and assuming a constant rate of removal for each dosing period). There was a general, although not consistent, trend for removal rates to be lower in the latter part of the experiment (i.e. after day 35) than in the earlier part (Figure 1).

Nutrient removal performance

Phosphate levels from full-scale WWTP effluents are legally regulated. The laboratory SBR was operating for biological phosphorus removal and thus this formed the basis for monitoring reactor function. Effluent $P\text{-}PO_4^{-3}$ levels during the 40-day pre-pandemic simulation period and first 21 days of the simulated pandemic (i.e., 0.1% and 1% OC dosing) were between 2 and 7 mg L^{-1} (Figure 2). Notably, effluent $P\text{-}PO_4^{-3}$ levels decreased to less than 1.2 mg L^{-1} by day 28, indicating a well-functioning reactor. However, from day 33 at the beginning of the 100% OC-only dosing, effluent $P\text{-}PO_4^{-3}$ values became erratic and were typically high, reaching a maximum of 34 mg L^{-1}, indicating reduced EBPR performance. This reduced EBPR during the dosing period was confirmed by other measures of performance. Firstly, the anaerobic phosphate release (Figure S2; used by others previously as a measure of EBPR performance; He et al., 2008, Slater et al., 2010, Zilles et al., 2002). Secondly, complete anaerobic consumption of acetate, which occurred for the 40-day pre-pandemic period and throughout the simulated pandemic period, failed on day 56, when consumption became incomplete (data not shown). Thirdly, nitrification (which occurred despite the operation of the SBR primarily for EBPR), as evidenced by aerobic nitrate production (Figure S3) decreased from over 0.85 mg $N\text{-}NO_3^-$ g^{-1} VSS for the pre-pandemic

period and the first 35 days of simulated pandemic to below 0.4 mg $N\text{-}NO_3^-$ g^{-1} VSS at the end of the 100% OC dosing period.

Granule structure

The mixed liquor suspended solids (MLSS; equivalent to cell dry weight) in the SBR was between 12.68 and 15.12 g L^{-1} from 7 days before dosing to day 56 (data not shown). Granule particle size distribution was between approximately 80 µm (10^{th} percentile) and 1320 µm (90^{th} percentile), with a median granule size of approximately 620 µm (Figure S4). Neither of these measures showed significant trends over the experiment. However, there were indications from light microscopy that some of the granules lost some structural integrity during the dosing as there was an appearance of fluffier material at days 49 and 58 (Figure S5). Additionally, there was evidence of an increase in the effluent SS from approximately 100 mg L^{-1} before dosing to approximately 400 mg L^{-1} on days 42 and 56 (Figure S6), suggesting sludge settling was poorer due to granule biofilm disruption.

Bacterial community structure

Diversity indices derived from 16S rRNA T-RFLP data indicated that there were changes in the community structure over the dosing period, with the Shannon diversity index decreasing over the last 14 days of dosing (Figure 3). This appeared to be a result of the development of a less even community structure (Figure S7) rather than the disappearance of particular operational taxonomic units (Figure S8). Whilst there was therefore some evidence of change in diversity indices, i.e. those describing aggregate community characteristics, there appeared to be little change in the relative abundance of two of the model organisms commonly found in EBPR systems. The relative abundance of a key organism responsible for EBPR, *Candidatus* "Accumulibacter phosphatis" (Hesselmann et al., 1999), was 27.1 % on day 0 (92% congruency score) and 22.8% on day 42 (end of 100% OC dosing; 96% congruency score), as assessed by quantitative FISH. The relative abundance of a glycogen-

219 accumulating organism and known EBPR antagonist, *Candidatus* "Competibacter

220 phosphatis" (Crocetti et al., 2002), was below 1% on days 0 and 42.

DISCUSSION

This is the first study in which the removal of OC, microbial diversity, nutrient removal performance and granule structure has been tested in a simulated activated sludge system exposed to OC and ABs in pandemic-scenario dosing.

There was up to 41% removal of OC per 6 h SBR cycle, with the most successful removal occurring in the first 35 days of dosing. It may be that in a real pandemic scenario, 35 days of significant removal at the beginning of an epidemic would reduce the amount of OC released into receiving waters. However, during the SBR operation there was no evidence of significant OC removal after day 35. Hence, there does not appear to be sufficient selective pressure for the enrichment of OC-degraders in the system investigated.

There was no evidence of any adverse effects on reactor performance during the first 28 days of simulated pandemic (i.e. up to 36 μg L^{-1} OC, 70 μg L^{-1} amoxicillin, 30 μg L^{-1} erythromycin, and 10 μg L^{-1} levofloxacin). There was however evidence during and after the two-week high-OC dosing period (days 29 – 42; 360 μg L^{-1} OC) of a reduction in EBPR and nitrification, bacterial community diversity and disruption to granule structure. This evidence of ecotoxicity in a simulated WWTP complements, but also contrasts with other studies that found no OC toxicity in fresh water (Accinelli et al., 2010) and activated sludge performance (Straub, 2009; testing limited to COD removal only). The positioning of the high OC-only dosing period in the middle of the pandemic scenario (i.e. dosing of OC and ABs) meant that we were not able to completely differentiate the causes of the perturbation to community structure and function; however, it is clear from this study that WWTPs may experience reduced efficiency during an influenza pandemic owing to high concentrations of bioactive pharmaceuticals, such as antivirals and antibiotics.

The SBR chosen for this study had a relatively long history of stable EBPR performance (>6 months). EBPR failure has previously been shown to occur as a result of competition with

246 glycogen accumulating organisms (Bond et al., 1999) and from bacteriophage infection(Barr
247 et al., 2010) (Barr et al., 2010), hence, the loss in reactor function in this study might not be
248 due to pharmaceutical exposure. However, as quantitative FISH analyses did not
249 demonstrate a decrease in the relative abundance of *Candidatus* "Accumulibacter
250 phosphatis", as would be expected if bacterial competition or bacteriophage predation was to
251 blame, it was concluded that pharmaceutical exposure was the more likely cause. As the
252 SBR was operated as a granular (rather than floccular) sludge, it remains untested whether
253 floccular sludge would respond differently to such exposure. Granular sludge systems do
254 have some operational differences to floccular systems, such as longer sludge ages, higher
255 mixed liquor suspended solids and lower available surface area, all of which might affect
256 sludge-pharmaceutical interactions.
257 It was only after dosing high concentrations of ABs and OC that effects on EBPR
258 performance were noticed. Therefore, it may be that it is only under severe pandemic
259 scenarios that disruption to WWTPs is of concern. Nonetheless, this research highlights the
260 reality of this chemical risk to WWTP function and the need for additional mixed-
261 pharmaceutical dosing studies in WWTP systems. These will be important for optimising
262 WWTP operation to contend with threats to WWTP function, and for understanding and
263 modelling the release of pharmaceuticals to the environment.
264

265 **ACKNOWLEDGEMENTS**

266 We thank F. Hoffman-La Roche Ltd. for the kind donation of oseltamivir carboxylate and
267 Michael Poole for assistance with Figure S1. This work was funded by a UQ New Staff
268 Research Start-up Grant awarded to FRS and the Natural Environment Research Council –
269 Knowledge Transfer Initiative (PREPARE) contract no. NE/F009216/1 awarded to ACS. We
270 thank two anonymous reviewers for their comments on the text.
271

271 **Figure legends**

272

273 **Figure 1**. Effluent OC concentration, showing observed values (filled circles) and predicted
274 values assuming no degradation (open circles). Dotted lines represent the ends of a particular
275 dosing regime and indicate the OC dosing level as a percentage of the maximum dose.

276

277 **Figure 2**. Effluent P-PO_4^{-3} concentrations, from flow injection analysis (filled circles) and
278 colourimetric tests (open circles). Dotted lines represent the ends of a particular dosing
279 regime and indicate the OC dosing level as a percentage of the maximum dose.

280

281 **Figure 3**. Shannon diversity, *H*, derived from analysis of T-RFLP data. Dotted lines
282 represent the ends of a particular dosing regime and indicate the OC dosing level as a
283 percentage of the maximum dose.

284

285

285 **Figurel**

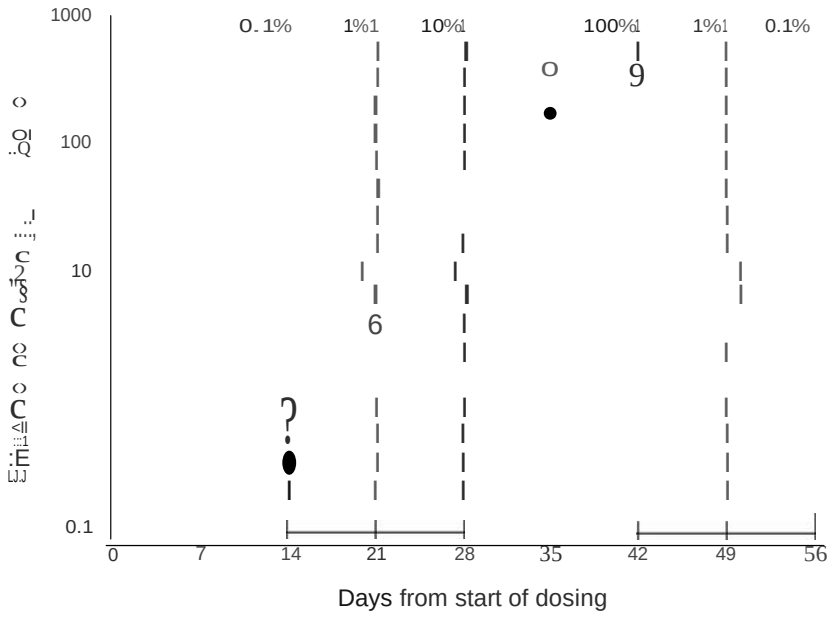

286

287

287 **Figure 2**

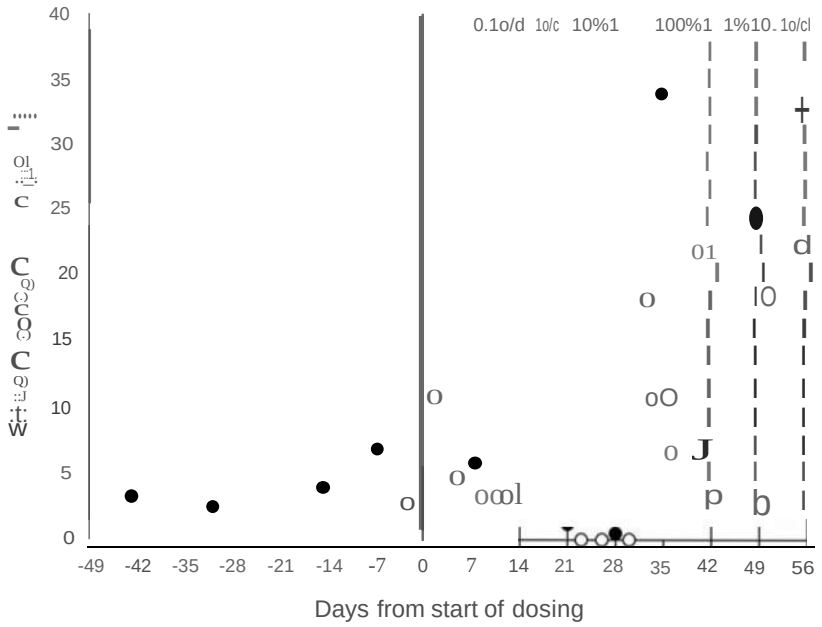

288

289

289 **Figure 3**

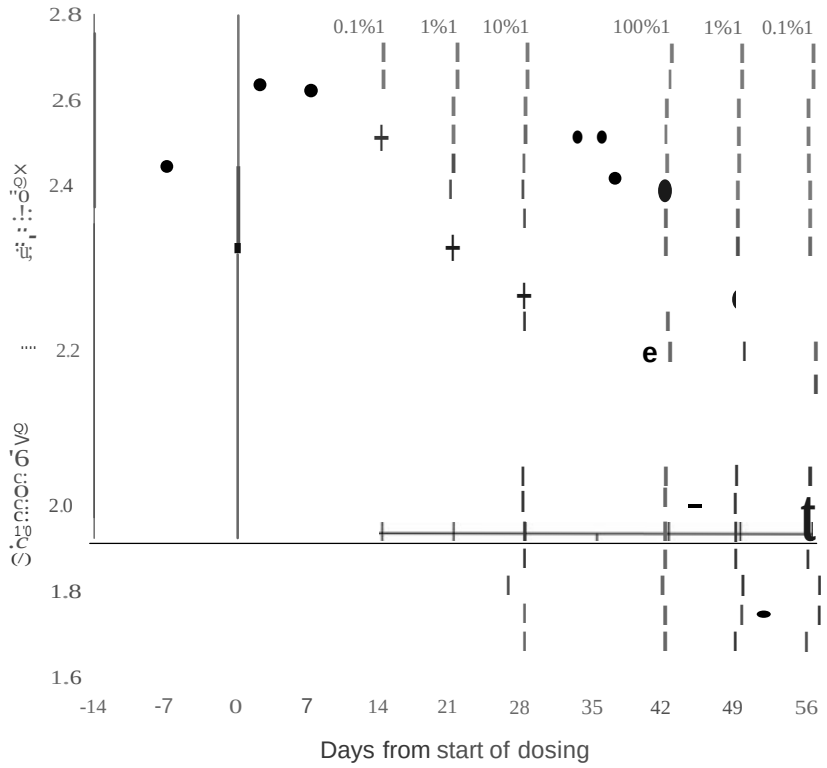

290

291

References

Accinelli, C., Caracciolo, A.B. and Grenni, P. (2007) Degradation of the antiviral drug oseltamivir carboxylate in surface water samples. International Journal of Environmental Analytical Chemistry 87(8), 579-587.

Accinelli, C., Sacca, M.L., Fick, J., Mencarelli, M., Lindberg, R. and Olsen, B. (2010) Dissipation and removal of oseltamivir (Tamiflu) in different aquatic environments. Chemosphere 79(8), 891-897.

Amann, R.I. (1995) Molecular Microbial Ecology Manual. Akkerman, A.D.L., Elsas, D.J.v. and Bruijn, F.J.D.o.d. (eds), pp. 1-15, Kluwer Academic Publishers.

APHA (1998) Standard Methods for the Examination of Water and Wastewater, American Public Health Association, Washington, DC.

Barr, J.J., Slater, F.R., Fukushima, T. and Bond, P.L. (2010) Evidence for bacteriophage activity causing community and performance changes in a phosphorus removal activated sludge. Fems Microbiology Ecology DOI:10.1111/j.1574-6941.2010.00967.x.

Bartels, P. and von Tumpling, W. (2008) The environmental fate of the antiviral drug oseltamivir carboxylate in different waters. Science of the Total Environment 405(1-3), 215-225.

Bond, P.L., Erhart, R., Wagner, M., Keller, J. and Blackall, L.L. (1999) Identification of some of the major groups of bacteria in efficient and nonefficient biological phosphorus removal activated sludge systems. Applied and Environmental Microbiology 65(9), 4077-4084.

Crocetti, G.R., Banfield, J.F., Keller, J., Bond, P.L. and Blackall, L.L. (2002) Glycogen-accumulating organisms in laboratory-scale and full-scale wastewater treatment processes. Microbiology-Sgm 148, 3353-3364.

Daughton, C.G. and Ternes, T.A. (1999) Pharmaceuticals and personal care products in the environment: Agents of subtle change? Environmental Health Perspectives 107, 907-938.

de Kreuk, M.K., Kishida, N. and van Loosdrecht, M.C.M. (2007) Aerobic granular sludge - state of the art. Water Science and Technology 55(8-9), 75-81.

Fick, J., Lindberg, R., Tysklind, M., Haemig, P.D., Walderstrom, J., Wallensten, A. and Olsen, B. (2007) Antiviral Oseltamivir is not removed or degraded in normal sewage water treatment: Implications for development of resistance by Influenza A virus. PLoS One 2(10), Article No.: e986.

Ghosh, G.C., Nakada, N., Yamashita, N. and Tanaka, H. (2010) Oseltamivir Carboxylate, the Active Metabolite of Oseltamivir Phosphate (Tamiflu), Detected in Sewage Discharge and River Water in Japan. Environmental Health Perspectives 118(1), 103-107.

He, G., Massarella, J. and Ward, P. (1999) Clinical pharmacokinetics of the prodrug oseltamivir and its active metabolite Ro 64-0802. Clinical Pharmacokinetics 37(6), 471-484.

He, S., Gu, A.Z. and McMahon, K.D. (2008) Progress toward understanding the distribution of *Accumulibacter* among full-scale enhanced biological phosphorus removal systems. Microbial Ecology 55(2), 229-236.

Hesselmann, R.P.X., Werlen, C., Hahn, D., van der Meer, J.R. and Zehnder, A.J.B. (1999) Enrichment, phylogenetic analysis and detection of a bacterium that performs enhanced biological phosphate removal in activated sludge. Systematic and Applied Microbiology 22(3), 454-465.

Lim, W.S., Douglas, G., Honeybourne, D., Macfarlane, J., Woodhead, M., Read, R., Beeching, N., Nicholson, K., Bannister, B., Leese, J., George, R.C., Nguyen-Van-Tam, J.S., Thomson, A., Ajayiobe, E., Coote, N., Harnden, A., Heath, P., McKenzie, S., Little, P., Butler, C., Fahey, T., Fleming, D. and Francis, N. (2007) Pandemic flu: clinical management of patients with an influenza-like illness during an influenza pandemic. Thorax 62, 1-46.

Lu, H.B., Oehmen, A., Virdis, B., Keller, J. and Yuan, Z.G. (2006) Obtaining highly enriched cultures of *Candidatus* Accumulibacter phosphatis through alternating carbon sources. Water Research 40(20), 3838-3848.

Parker, D., Soong, G., Planet, P., Brower, J., Ratner, A.J. and Prince, A. (2009) The NanA neuraminidase of *Streptococcus pneumoniae* is involved in biofilm formation. Infection and Immunity 77(9), 3722-3730.

Prasse, C., Schlusener, M.P., Schulz, R. and Ternes, T.A. (2010) Antiviral Drugs in Wastewater and Surface Waters: A New Pharmaceutical Class of Environmental Relevance? Environmental Science & Technology 44(5), 1728-1735.

Sacca, M.L., Accinelli, C., Fick, J., Lindberg, R. and Olsen, B. (2009) Environmental fate of the antiviral drug Tamiflu in two aquatic ecosystems. Chemosphere 75(1), 28-33.

Seviour, R.J., Mino, T. and Onuki, M. (2003) The microbiology of biological phosphorus removal in activated sludge systems. Fems Microbiology Reviews 27(1), 99-127.

Singer, A.C., Nunn, M.A., Gould, E.A. and Johnson, A.C. (2007) Potential risks associated with the proposed widespread use of Tamiflu. Environmental Health Perspectives 115(1), 102-106.

Singer, A.C., Johnson, A.C., Anderson, P.D. and Snyder, S.A. (2008) Reassessing the risks of Tamiflu use during a pandemic to the Lower Colorado River. Environmental Health Perspectives 116(7), A285-A286.

Singer, A.C., Colizza, V., Schmitt, H., Andrews, J., Balcan, D., Huang, W.E., Keller, V.D.J., Vespignani, A. and Williams, R.J. (submitted) Assessing the sustainability and ecotoxicological risks of pandemic influenza medical response. Environmental Health Perspectives.

Slater, F.R., Johnson, C.R., Blackall, L.L., Beiko, R.G. and Bond, P.L. (2010) Monitoring associations between clade-level variation, overall community structure and ecosystem function in enhanced biological phosphorus removal (EBPR) systems using terminal-restriction fragment length polymorphism (T-RFLP). Water Research 44(17), 4908-4923.

Soderstrom, H., Jarhult, J.D., Fick, J., Lindberg, R., Singer, A.C., Grabic, R. and Olsen, B. (2010) Levels of antivirals and antibiotics in the river Thames, UK, during the pandemic 2009. SETAC Europe Annual Meeting.

Soong, G., Muir, A., Gomez, M.I., Waks, J., Reddy, B., Planet, P., Singh, P.K., Kanetko, Y., Wolfgang, M.C., Hsiao, Y.S., Tong, L. and Prince, A. (2006)

Bacterial neuraminidase facilitates mucosal infection by participating in biofilm production. Journal of Clinical Investigation 116(8), 2297-2305.

Straub, J.O. (2009) An environmental risk assessment for oseltamivir (Tamiflu®) for sewage works and surface waters under seasonal-influenza- and pandemic-use conditions. Ecotoxicology and Environmental Safety 72, 1625-1634.

Zilles, J.L., Peccia, J., Kim, M.W., Hung, C.H. and Noguera, D.R. (2002) Involvement of *Rhodocyclus*-related organisms in phosphorus removal in full-scale wastewater treatment plants. Applied and Environmental Microbiology 68(6), 2763-2769.

Supplementary Information

Pandemic pharmaceutical dosing effects on wastewater treatment: no adaptation of activated sludge bacteria to degrade the antiviral drug Oseltamivir (Tamiflu) and loss of nutrient removal performance

Slater, F.R.[1], Singer, A.C.[2], Turner, S.[3], Barr, J.J.[1] & Bond, P.L. [1*]

For submission to FEMS Microbiology Letters

Reactor Operation

The synthetic feed introduced to the SBR at the beginning of each cycle comprised approximately 0.6 L solution A (autoclaved) and 1.3 L solution B. Solution A contained (g L^{-1} unless otherwise stated): NH_4Cl (1.02), peptone (0.014), yeast (0.014), $MgSO_4.7H_20$ (5.48), $CaCl_2.2H_20$ (0.588), nutrient solution after Smolders et al. (1994) (1 mL), allyl-n thiourea (ATU, a nitrification inhibitor; 0.014) and *either* $NaCH_3COO.3H_20$ (8.5) *or* CH_3CH_2COOH (2.646 mL) and 2M NaOH (8 mL) to provide identical mg COD L^{-1}. Solution B contained (g L^{-1}): K_2HPO_4 (0.132), KH_2PO_4 (0.103) and 2M NaOH (1.6 mL). Each cycle was 6 h, with a draw and fill (36 mins), an anaerobic phase (90), aerobic phase (232), waste (1), settle (1). The SBR was operated stably for EBPR for a period of 6 months before dosing, with effluent P concentrations consistently below 7 mg L^{-1}.

Oseltamivir Carboxylate (OC) measurement

The OC concentration in the samples was determined by high performance liquid chromatography tandem mass spectrometry (LCMSMS). The system used was an Agilent 1200 HPLC system coupled to the Agilent 6410B triple quadrupole mass spectrometer. 50 µL of the aqueous samples was injected onto an ACE C18 column (2.1 mm i.d. × 150 mm length, 3 µm particle size) held at 45 ^{o}C. The mobile phase was 0.1% formic acid in deionised water (solvent A) and 0.1% formic acid in methanol (solvent B) starting at 15% solvent B and with the following solvent gradient at a flow rate of 0.3 mL min^{-1}:

Time (mins)	Solvent B (%)
0.00	15
10.00	70
10.50	100
11.50	100
12.00	15

Postime/equilibration time: 10 mins

The Agilent triple quadrupole mass spectrometer was operated in positive electrospray ionisation mode. The nebuliser pressure, dry gas flow, dry gas temperature and Capillary voltage were held constant at 60 psig, 12 L min^{-1}, 350 ^{o}C and 5000 V respectively. Data was acquired in multiple reaction monitoring mode monitoring the 285.1 → 197.1 and 285.1 → 138.1 transitions with collision energies of 4 V and 16 V respectively and a fragmentor voltage of 90 V. To check the performance of the method with real matrix samples a spike recovery was performed on surface water spiked at 30 ppb and 1000 ppb which returned recoveries of 110% and 107% and RSDs of 6.3% and 3% respectively (n = 5). To check that there was consistent recovery over a range of relevant concentrations, a series of 10-fold dilutions of OC, from 0.018 to 1800 µg L^{-1} OC, in sterile distilled water were measured. All were within 9.7% of their predicted values. The limit of detection was 0.01 µg L^{-1}.

Biochemical analyses

Ammonium ($N\text{-}NH_4^+$), nitrate ($N\text{-}NO_3^-$), nitrite ($N\text{-}NO_2^-$), orthophosphate ($P\text{-}PO_4^{3-}$) were measured using either a Lachat QuikChem8000 flow injection analyser or, for P- PO_4^{3-} only, a Reflectoquant® P test (5-20 mg PO_4^{3-} L^{-1}; Merck KGaA, Darmstadt, Germany). Acetate concentrations were measured using an Agilent 7890A gas chromatograph (GC) with a FID detector and a Phenomenex ZB-FFAP column (30 m × 0.53 mm × 1.0 µm).

T-RFLP

Genomic DNA was subjected to PCR using the primers 63F (5' FAM (6-carboxyfluorescein) -labelled) and 1389R (Marchesi et al., 1998) and the purified PCR products subjected to digestion using the restriction enzyme MspI. Digested products were ethanol precipitated and sent to the Australian Genome Research Facility (Glen Osmond, SA, Australia) to be analysed on an AB3730 Genetic Bioanalyzer (Applied Biosystems, Foster City, CA, USA) fitted with a 36 cm array and using the GS500(-250)LIZ standard. Data was processed and standardised and calculations of diversity indices, including Richness (*S*), the Shannon Diversity Index (*H*), and Shannon Evenness (*J*), were made as before (Slater et al., 2010) .

Fluorescence *in situ* hybridisation (FISH)

EUBMIX (Daims et al., 1999) was used to target all bacteria, PAOMIX (Crocetti et al., 2000) was used to target *Candidatus* "Accumulibacter phosphatis", and GAOQ989 (Crocetti et al., 2002) and GBG2 (Kong et al., 2002) were used in conjunction to target *Candidatus* "Competibacter phosphatis". The slides were viewed and images captured using a Zeiss LSM 510 Meta confocal laser scanning microscope (CLSM) using a Zeiss Neofluar × 40/1.3 oil objective. Images were analysed using *daime* version 1.3.1 (Daims et al., 2006), with image segmentation carried out using default parameters. Biovolumes were calculated from

over 30 images acquired from 4 different wells of a slide using the biovolume fraction function *(daime* user manual; http://www.microbial-ecology.net/daime/daime-manual.asp). The artefact rejection tool was set at a congruency threshold of 75%.

Table S1. Dosing of pharmaceuticals. N.B. Only OC was measured; the measured concentrations of OC were within 16% of their expected values for all except the lowest dose (i.e. 0.36 µg OC L^{-1} or 0.1% of the maximum dose), for which the measured values were different by between 27 and 75% of their expected values.

Days from start of dosing	**Dosing of pharmaceuticals in influent wastewater (µg L^{-1})**			
	OC	**Amoxicillin**	**Erythromycin**	**Levofloxacin**
1-7	0.36	0.7	0.3	0.1
8-14	0.36	0.7	0.3	0.1
15-21	3.6	7	3	1
22-28	36	70	30	10
29-35	360	0	0	0
36-42	360	0	0	0
43-49	3.6	7	3	1
50-56	0.36	0.7	0.3	0.1

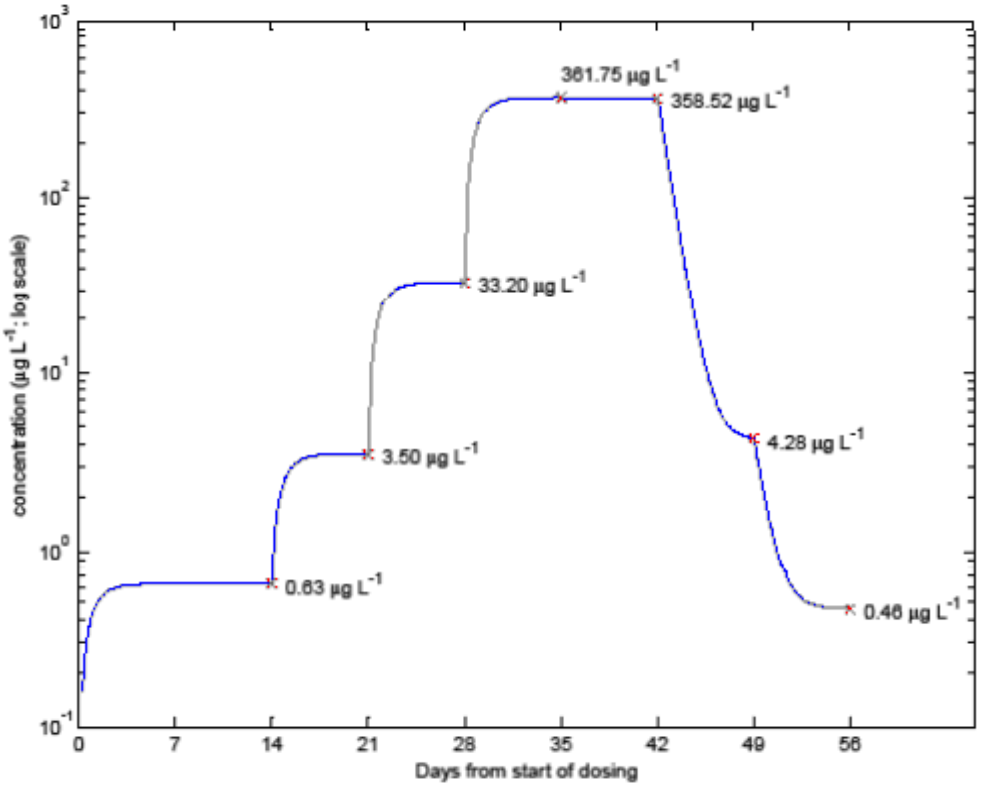

Figure S1. Simulated effluent OC concentrations based on measured influent OC concentrations and four SBR draw and fill occurrences per day, each with a volumetric exchange ratio of 1:4, and assuming no sorption or biological transformation (i.e. no removal of OC) by sludge.

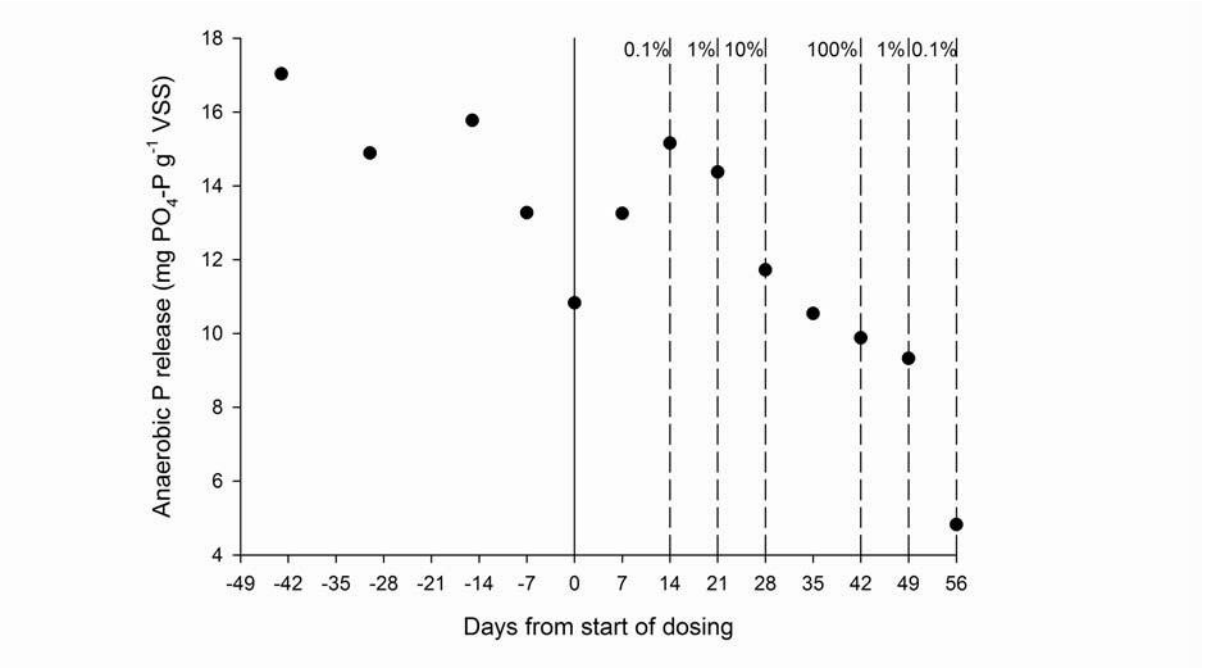

Figure S2. Anaerobic $P\text{-}PO_4^{-3}$ release (normalised to volatile suspended solids (VSS); analogous to cell dry weight). Whilst anaerobic release averaged greater than 13.5 mg $P\text{-}PO_4^{-3}$ g^{-1} VSS for the 40 day pre-pandemic period and first 21 days of the simulated pandemic period, it went below 10 mg $P\text{-}PO_4^{-3}$ g^{-1} VSS in the 100% OC dosing period and had decreased to below 5 mg $P\text{-}PO_4^{-3}$ g^{-1} VSS by the end of the dosing period. Dotted lines represent the ends of a particular dosing regime and indicate the OC dosing level as a percentage of the maximum OC dose.

.

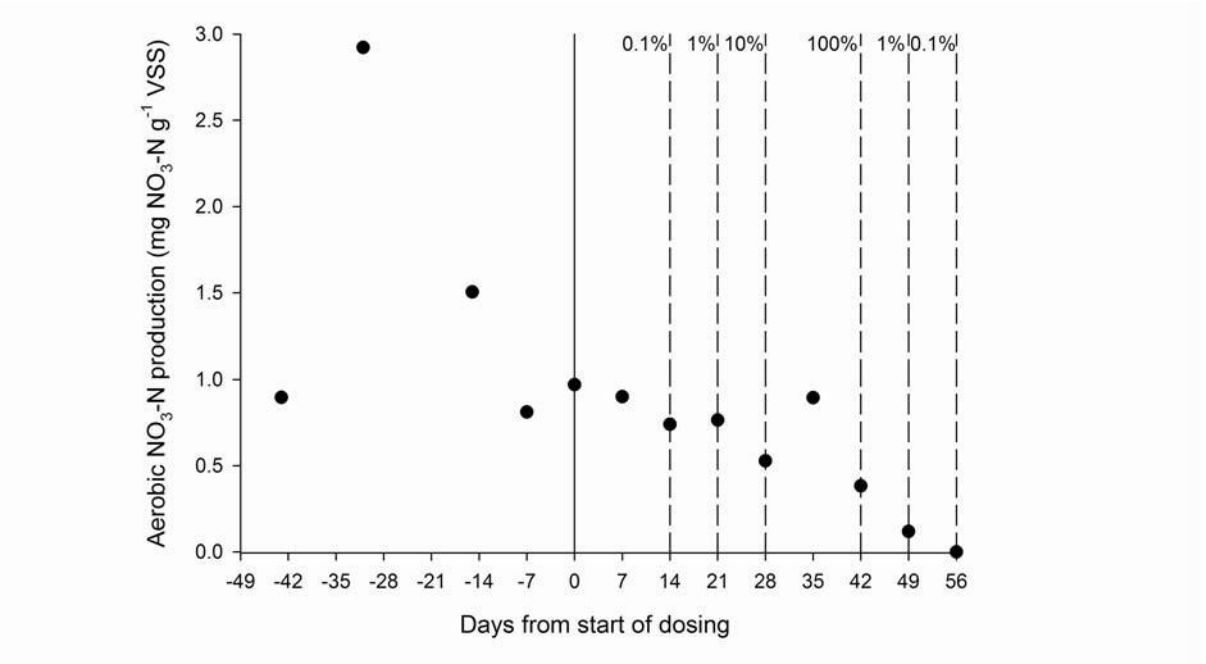

Figure S3. Aerobic nitrate production (normalised to volatile suspended solids (VSS); analogous to cell dry weight). Whilst aerobic nitrate production averaged over 0.85 mg N-NO_3^- g^{-1} VSS for the pre-pandemic period and the first 35 days of simulated pandemic period (excluding outlier at 31 days before start of dosing), it had decreased to below 0.4 mg N-NO_3^- g^{-1} VSS by day 42 and there was no nitrate production by day 56. Dotted lines represent the ends of a particular dosing regime and indicate the OC dosing level as a percentage of the maximum dose.

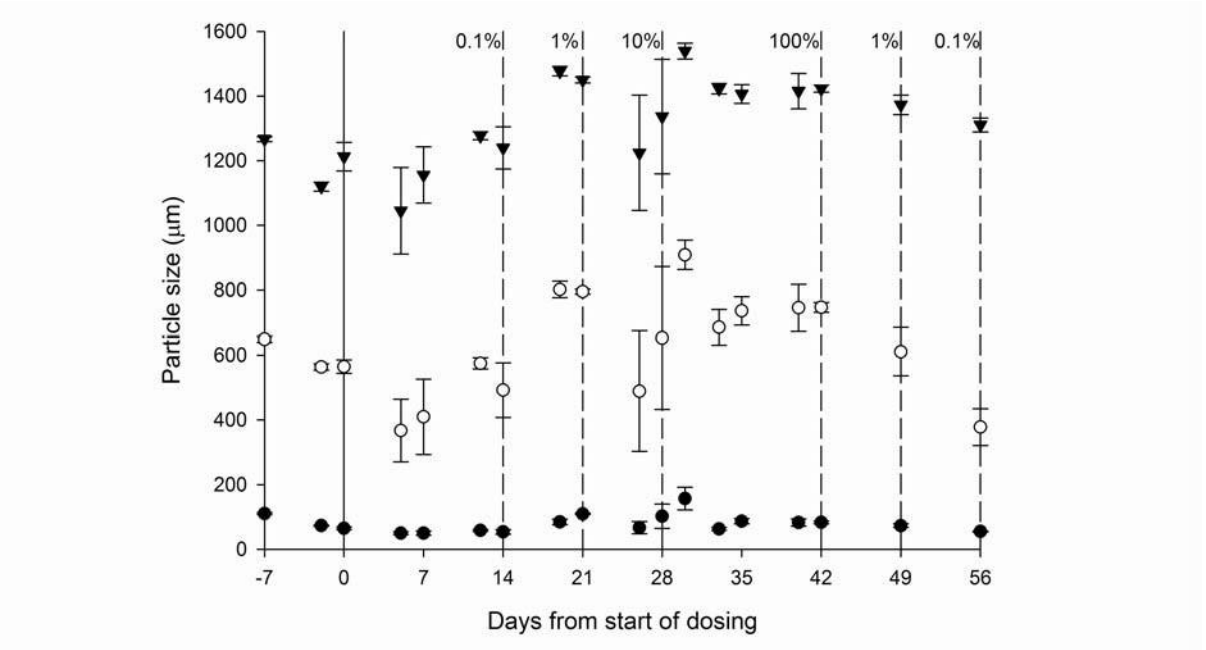

Figure S4. Particle size distribution of granules, including 10th (filled circles), 50th (open circles) and 90th (filled triangles) percentiles. Error bars represent standard error of the mean of three replicate measurements. Dotted lines represent the ends of a particular dosing regime and indicate the OC dosing level as a percentage of the maximum dose.

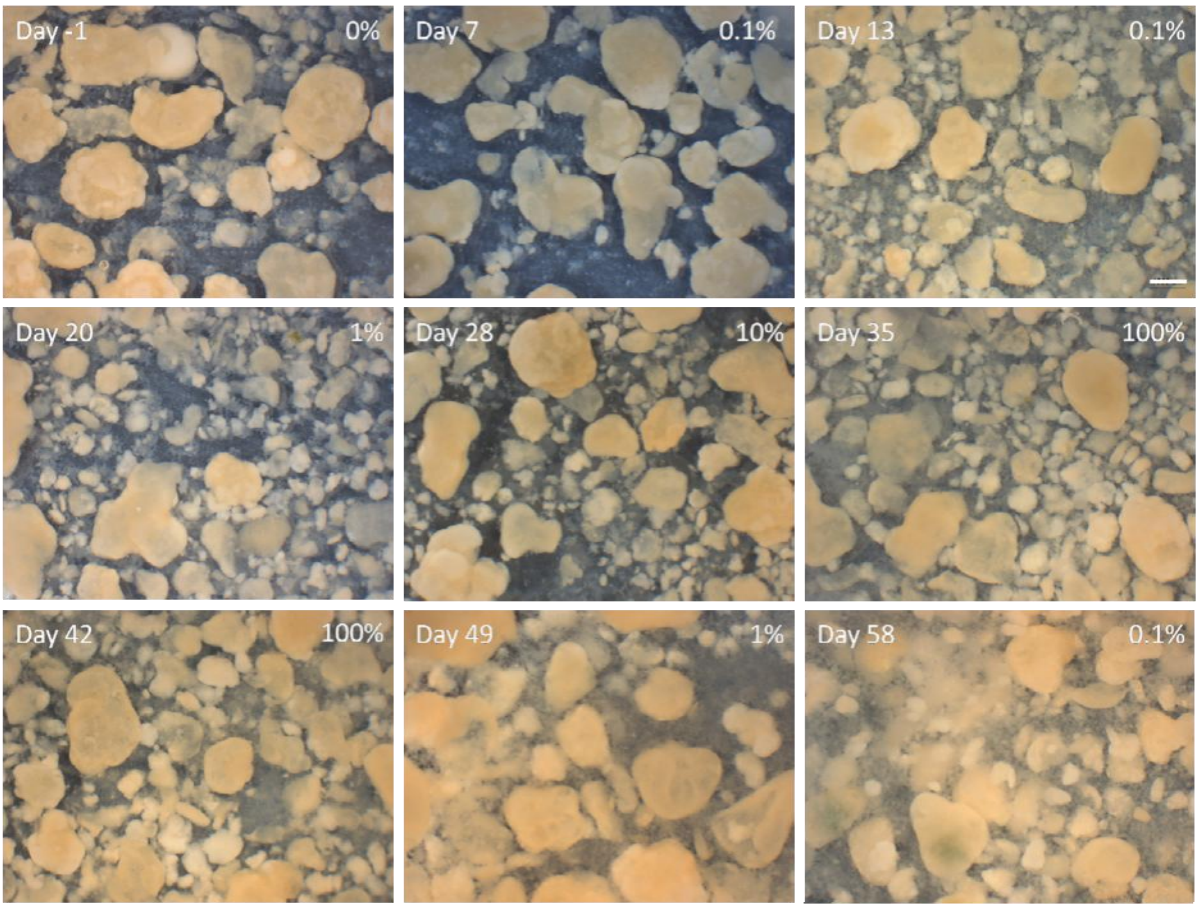

Figure S5. Light microscopy images of granules against a black background taken on different days at different dosing regimes (indicated as the OC dosing level as a percentage of the maximum dose). All images were taken at the same magnification. Scale bar (Day 13 image) represents 1500 µm.

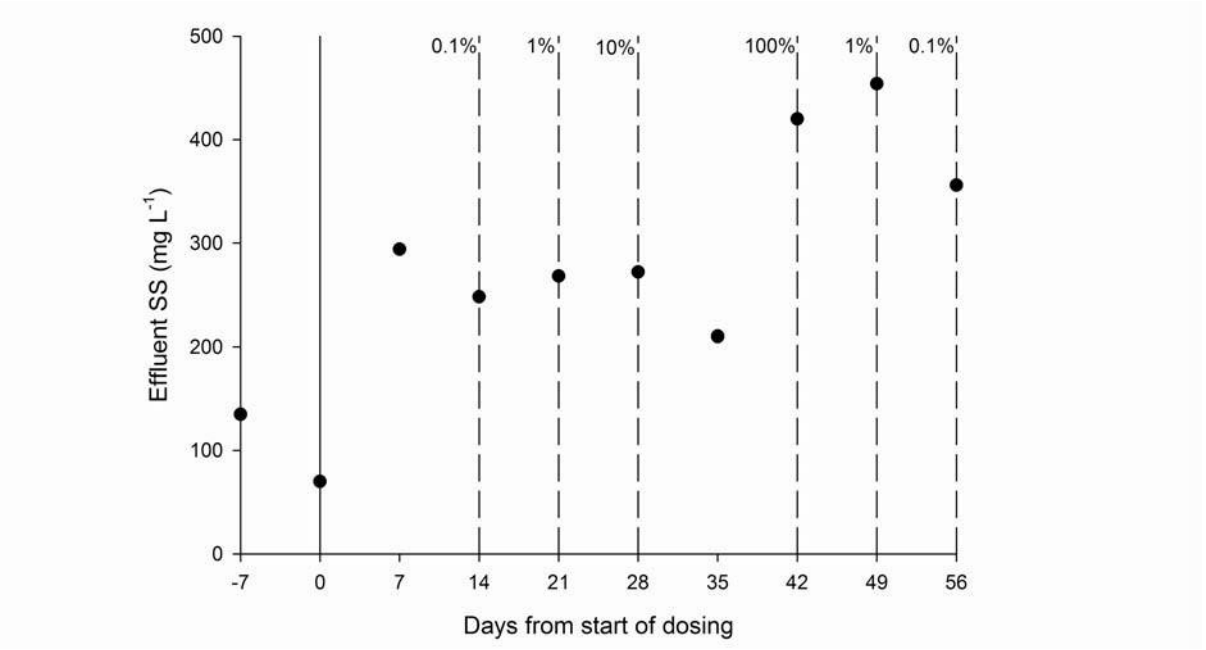

Figure S6. Effluent suspended solids (SS). Dotted lines represent the ends of a particular dosing regime and indicate the OC dosing level as a percentage of the maximum dose.

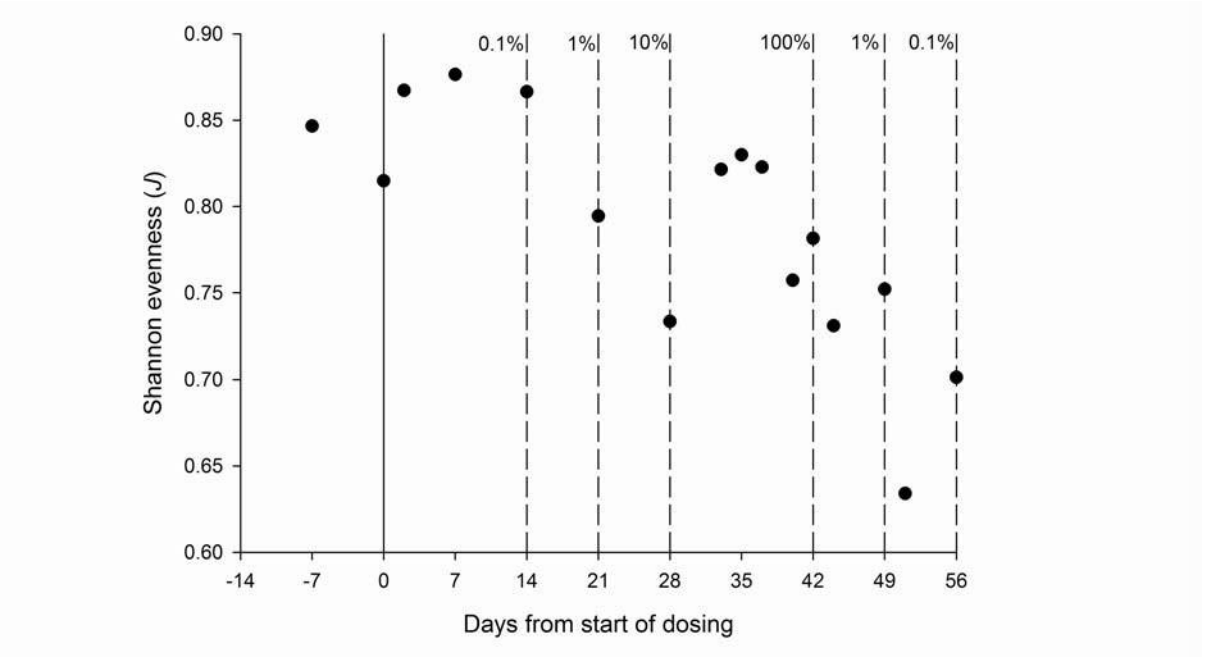

Figure S7. Shannon evenness (*J*) derived from T-RFLP data. Dotted lines represent the ends of a particular dosing regime and indicate the OC dosing level as a percentage of the maximum dose.

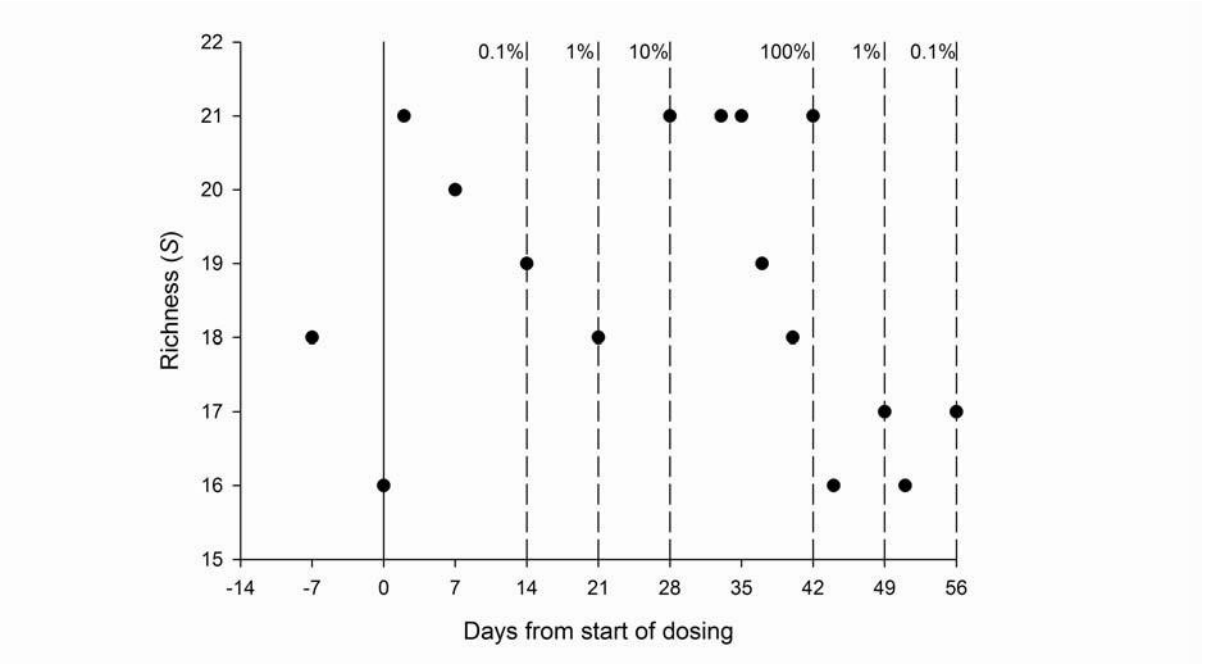

Figure S8. Richness (*S*) derived from T-RFLP data. Dotted lines represent the ends of a particular dosing regime and indicate the OC dosing level as a percentage of the maximum dose.

References

Crocetti, G.R., Hugenholtz, P., Bond, P.L., Schuler, A., Keller, J., Jenkins, D. and Blackall, L.L. (2000) Identification of polyphosphate-accumulating organisms and design of 16S rRNA-directed probes for their detection and quantitation. Applied and Environmental Microbiology 66(3), 1175-1182.

Crocetti, G.R., Banfield, J.F., Keller, J., Bond, P.L. and Blackall, L.L. (2002) Glycogen-accumulating organisms in laboratory-scale and full-scale wastewater treatment processes. Microbiology-Sgm 148, 3353-3364.

Daims, H., Bruhl, A., Amann, R., Schleifer, K.H. and Wagner, M. (1999) The domain-specific probe EUB338 is insufficient for the detection of all Bacteria: Development and evaluation of a more comprehensive probe set. Systematic and Applied Microbiology 22(3), 434-444.

Daims, H., Lucker, S. and Wagner, M. (2006) *daime*, a novel image analysis program for microbial ecology and biofilm research. Environmental Microbiology 8(2), 200-213.

Kong, Y.H., Ong, S.L., Ng, W.J. and Liu, W.T. (2002) Diversity and distribution of a deeply branched novel proteobacterial group found in anaerobic-aerobic activated sludge processes. Environmental Microbiology 4(11), 753-757.

Marchesi, J.R., Sato, T., Weightman, A.J., Martin, T.A., Fry, J.C., Hiom, S.J. and Wade, W.G. (1998) Design and evaluation of useful bacterium-specific PCR primers that amplify genes coding for bacterial 16S rRNA. Applied and Environmental Microbiology 64(2), 795-799.

Slater, F.R., Johnson, C.R., Blackall, L.L., Beiko, R.G. and Bond, P.L. (2010) Monitoring associations between clade-level variation, overall community structure and ecosystem function in enhanced biological phosphorus removal (EBPR) systems using terminal-restriction fragment length polymorphism (T-RFLP). Water Research 44(17), 4908-4923.

Smolders, G.J.F., Vandermeij, J., Vanloosdrecht, M.C.M. and Heijnen, J.J. (1994) Model of the anaerobic metabolism of the biological phosphorus removal process - stoichiometry and pH influence. Biotechnology and Bioengineering 43(6), 461-470.

Supplementary Information

Pandemic pharmaceutical dosing effects on wastewater treatment: no adaptation of activated sludge bacteria to degrade the antiviral drug Oseltamivir (Tamiflu) and loss of nutrient removal performance

Slater, F.R.[1], Singer, A.C.[2], Turner, S.[3], Barr, J.J.[1] & Bond, P.L. [1*]

For submission to FEMS Microbiology Letters

Reactor Operation

The synthetic feed introduced to the SBR at the beginning of each cycle comprised approximately 0.6 L solution A (autoclaved) and 1.3 L solution B. Solution A contained (g L^{-1} unless otherwise stated): NH_4Cl (1.02), peptone (0.014), yeast (0.014), $MgSO_4.7H_20$ (5.48), $CaCl_2.2H_20$ (0.588), nutrient solution after Smolders et al. (1994) (1 mL), allyl-n thiourea (ATU, a nitrification inhibitor; 0.014) and *either* $NaCH_3COO.3H_20$ (8.5) *or* CH_3CH_2COOH (2.646 mL) and 2M NaOH (8 mL) to provide identical mg COD L^{-1}. Solution B contained (g L^{-1}): K_2HPO_4 (0.132), KH_2PO_4 (0.103) and 2M NaOH (1.6 mL). Each cycle was 6 h, with a draw and fill (36 mins), an anaerobic phase (90), aerobic phase (232), waste (1), settle (1). The SBR was operated stably for EBPR for a period of 6 months before dosing, with effluent P concentrations consistently below 7 mg L^{-1}.

Oseltamivir Carboxylate (OC) measurement

The OC concentration in the samples was determined by high performance liquid chromatography tandem mass spectrometry (LCMSMS). The system used was an Agilent 1200 HPLC system coupled to the Agilent 6410B triple quadrupole mass spectrometer. 50 µL of the aqueous samples was injected onto an ACE C18 column (2.1 mm i.d. × 150 mm length, 3 µm particle size) held at 45 ^oC. The mobile phase was 0.1% formic acid in deionised water (solvent A) and 0.1% formic acid in methanol (solvent B) starting at 15% solvent B and with the following solvent gradient at a flow rate of 0.3 mL min^{-1}:

Time (mins)	Solvent B (%)
0.00	15
10.00	70
10.50	100
11.50	100
12.00	15

Postime/equilibration time: 10 mins

The Agilent triple quadrupole mass spectrometer was operated in positive electrospray ionisation mode. The nebuliser pressure, dry gas flow, dry gas temperature and Capillary voltage were held constant at 60 psig, 12 L min^{-1}, 350 ^{o}C and 5000 V respectively. Data was acquired in multiple reaction monitoring mode monitoring the 285.1 → 197.1 and 285.1 → 138.1 transitions with collision energies of 4 V and 16 V respectively and a fragmentor voltage of 90 V. To check the performance of the method with real matrix samples a spike recovery was performed on surface water spiked at 30 ppb and 1000 ppb which returned recoveries of 110% and 107% and RSDs of 6.3% and 3% respectively (n = 5). To check that there was consistent recovery over a range of relevant concentrations, a series of 10-fold dilutions of OC, from 0.018 to 1800 µg L^{-1} OC, in sterile distilled water were measured. All were within 9.7% of their predicted values. The limit of detection was 0.01 µg L^{-1}.

Biochemical analyses

Ammonium ($N\text{-}NH_4^+$), nitrate ($N\text{-}NO_3^-$), nitrite ($N\text{-}NO_2^-$), orthophosphate ($P\text{-}PO_4^{3-}$) were measured using either a Lachat QuikChem8000 flow injection analyser or, for P- PO_4^{3-} only, a Reflectoquant® P test (5-20 mg PO_4^{3-} L^{-1}; Merck KGaA, Darmstadt, Germany). Acetate concentrations were measured using an Agilent 7890A gas chromatograph (GC) with a FID detector and a Phenomenex ZB-FFAP column (30 m × 0.53 mm × 1.0 µm).

T-RFLP

Genomic DNA was subjected to PCR using the primers 63F (5' FAM (6-carboxyfluorescein) -labelled) and 1389R (Marchesi et al., 1998) and the purified PCR products subjected to digestion using the restriction enzyme MspI. Digested products were ethanol precipitated and sent to the Australian Genome Research Facility (Glen Osmond, SA, Australia) to be analysed on an AB3730 Genetic Bioanalyzer (Applied Biosystems, Foster City, CA, USA) fitted with a 36 cm array and using the GS500(-250)LIZ standard. Data was processed and standardised and calculations of diversity indices, including Richness (*S*), the Shannon Diversity Index (*H*), and Shannon Evenness (*J*), were made as before (Slater et al., 2010) .

Fluorescence *in situ* hybridisation (FISH)

EUBMIX (Daims et al., 1999) was used to target all bacteria, PAOMIX (Crocetti et al., 2000) was used to target *Candidatus* "Accumulibacter phosphatis", and GAOQ989 (Crocetti et al., 2002) and GBG2 (Kong et al., 2002) were used in conjunction to target *Candidatus* "Competibacter phosphatis". The slides were viewed and images captured using a Zeiss LSM 510 Meta confocal laser scanning microscope (CLSM) using a Zeiss Neofluar × 40/1.3 oil objective. Images were analysed using *daime* version 1.3.1 (Daims et al., 2006), with image segmentation carried out using default parameters. Biovolumes were calculated from

over 30 images acquired from 4 different wells of a slide using the biovolume fraction function *(daime* user manual; http://www.microbial-ecology.net/daime/daime-manual.asp). The artefact rejection tool was set at a congruency threshold of75%.

Table S1. Dosing of pharmaceuticals. N.B. Only OC was measured; the measured concentrations of OC were within 16% of their expected values for all except the lowest dose (i.e. 0.36 µg OC L^{-1} or 0.1% of the maximum dose), for which the measured values were different by between 27 and 75% of their expected values.

Days from start of dosing	**Dosing of pharmaceuticals in influent wastewater (µg L^{-1})**			
	OC	**Amoxicillin**	**Erythromycin**	**Levofloxacin**
1-7	0.36	0.7	0.3	0.1
8-14	0.36	0.7	0.3	0.1
15-21	3.6	7	3	1
22-28	36	70	30	10
29-35	360	0	0	0
36-42	360	0	0	0
43-49	3.6	7	3	1
50-56	0.36	0.7	0.3	0.1

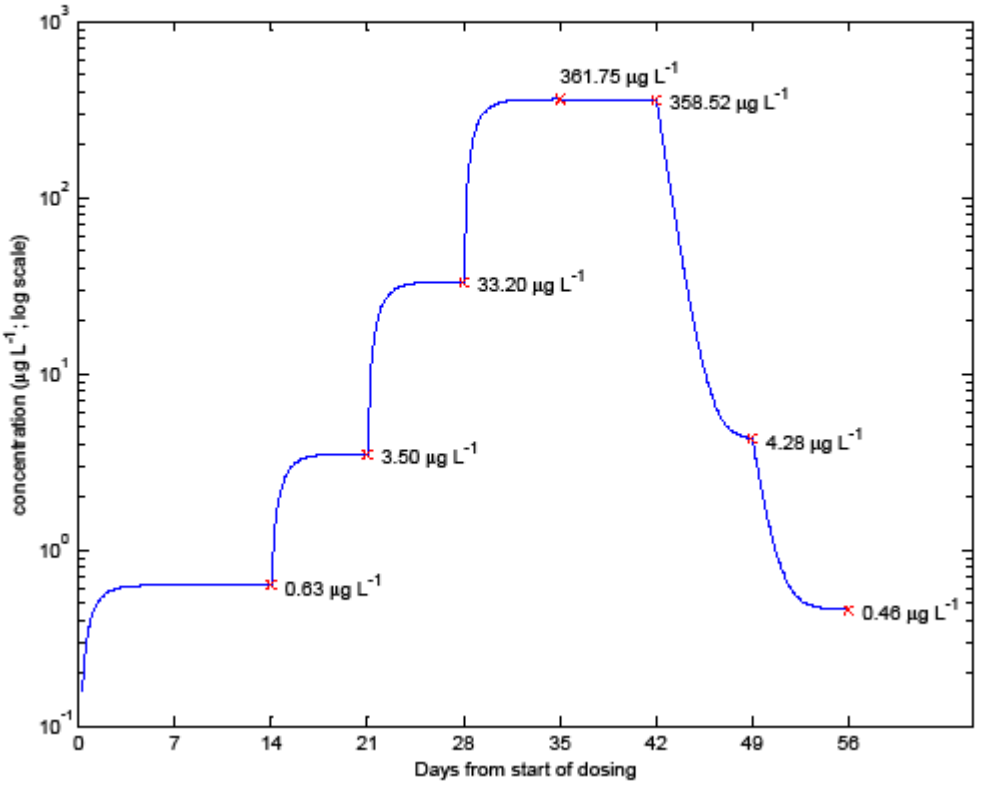

Figure S1. Simulated effluent OC concentrations based on measured influent OC concentrations and four SBR draw and fill occurrences per day, each with a volumetric exchange ratio of 1:4, and assuming no sorption or biological transformation (i.e. no removal of OC) by sludge.

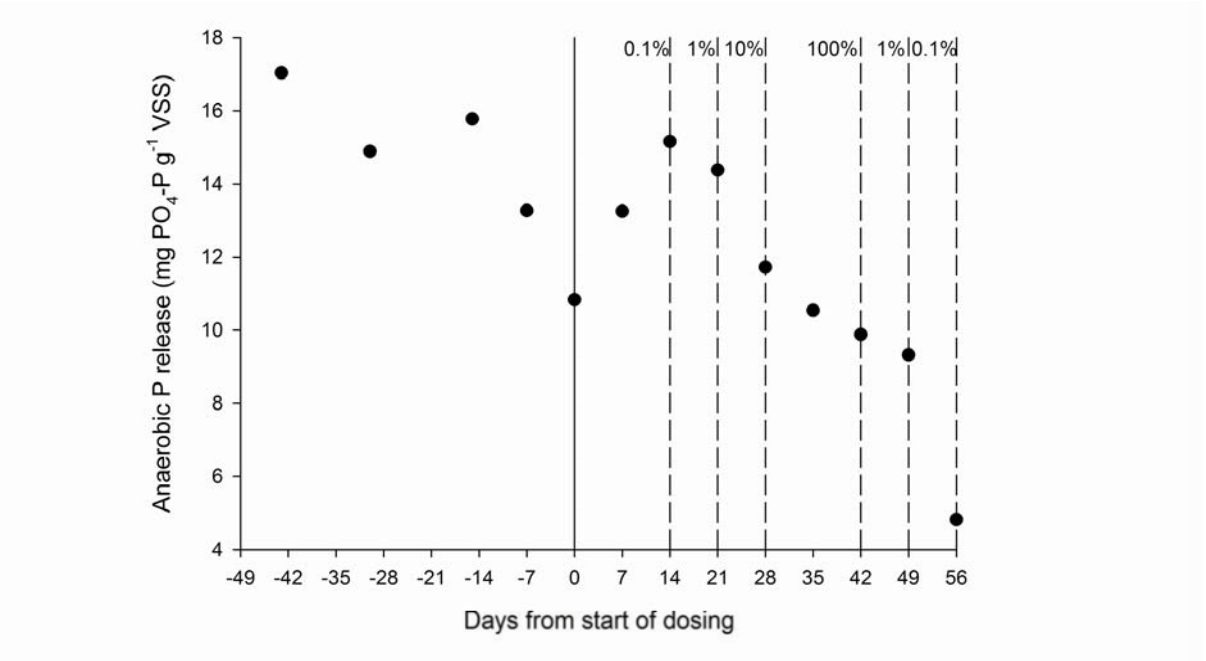

Figure S2. Anaerobic $P\text{-}PO_4^{-3}$ release (normalised to volatile suspended solids (VSS); analogous to cell dry weight). Whilst anaerobic release averaged greater than 13.5 mg $P\text{-}PO_4^{-3}$ g^{-1} VSS for the 40 day pre-pandemic period and first 21 days of the simulated pandemic period, it went below 10 mg $P\text{-}PO_4^{-3}$ g^{-1} VSS in the 100% OC dosing period and had decreased to below 5 mg $P\text{-}PO_4^{-3}$ g^{-1} VSS by the end of the dosing period. Dotted lines represent the ends of a particular dosing regime and indicate the OC dosing level as a percentage of the maximum OC dose.

.

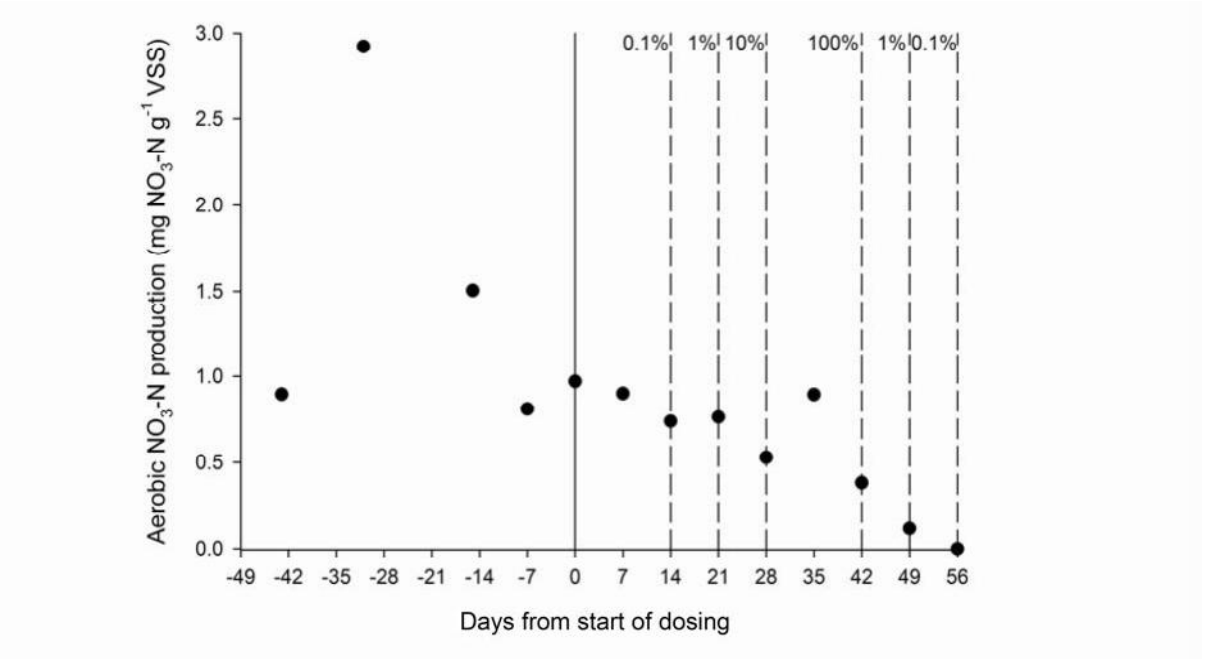

Figure S3. Aerobic nitrate production (normalised to volatile suspended solids (VSS); analogous to cell dry weight). Whilst aerobic nitrate production averaged over 0.85 mg N-NO_3^- g^{-1} VSS for the pre-pandemic period and the first 35 days of simulated pandemic period (excluding outlier at 31 days before start of dosing), it had decreased to below 0.4 mg N-NO_3^- g^{-1} VSS by day 42 and there was no nitrate production by day 56. Dotted lines represent the ends of a particular dosing regime and indicate the OC dosing level as a percentage of the maximum dose.

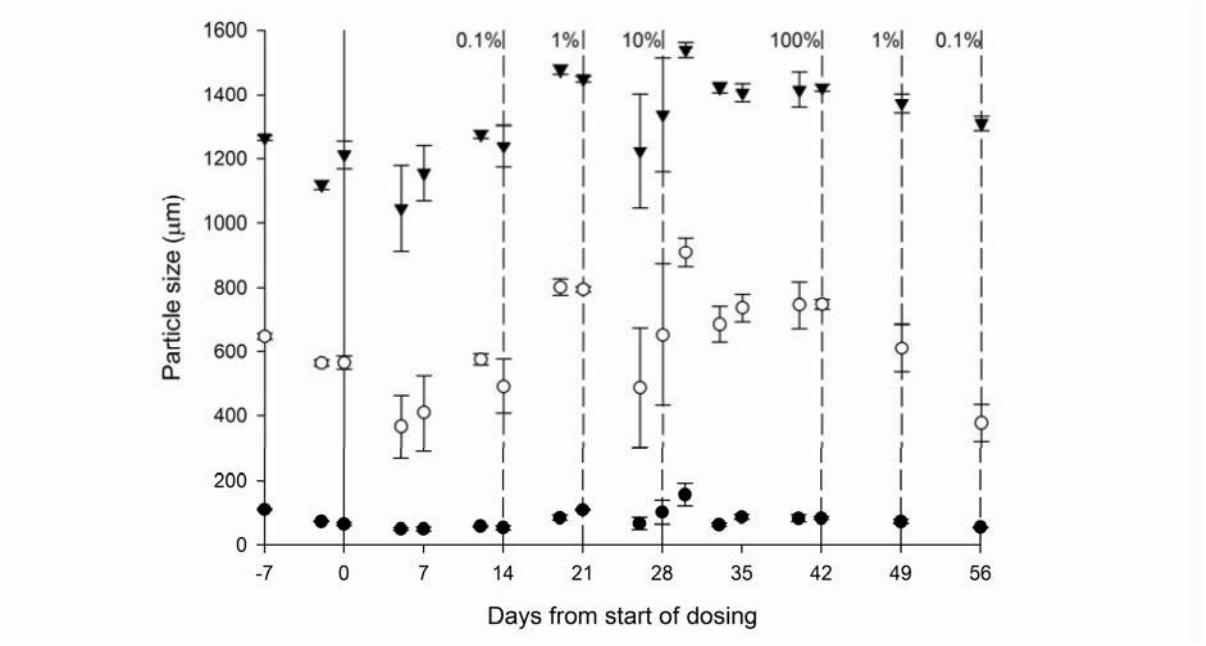

Figure S4. Particle size distribution of granules, including 10th (filled circles), 50th (open circles) and 90th (filled triangles) percentiles. Error bars represent standard error of the mean of three replicate measurements. Dotted lines represent the ends of a particular dosing regime and indicate the OC dosing level as a percentage of the maximum dose.

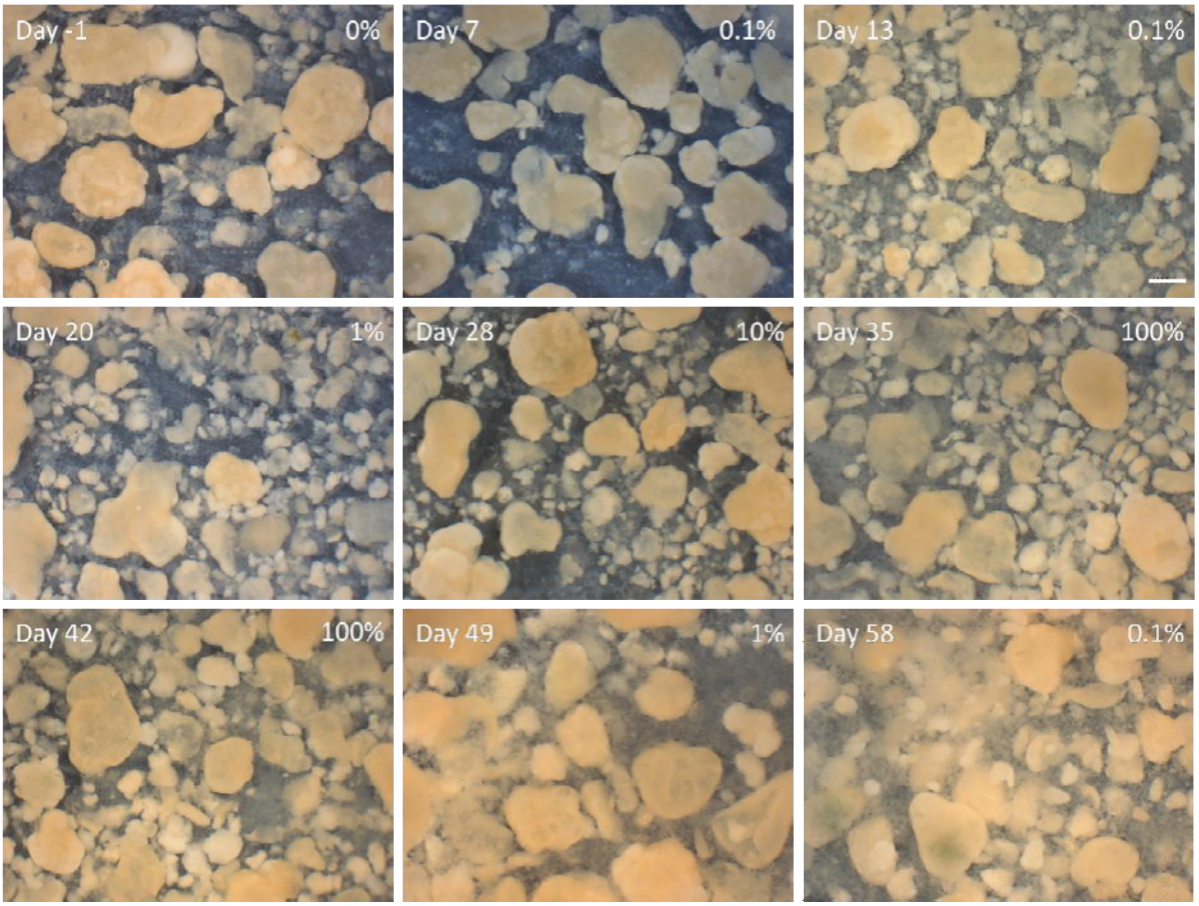

Figure S5. Light microscopy images of granules against a black background taken on different days at different dosing regimes (indicated as the OC dosing level as a percentage of the maximum dose). All images were taken at the same magnification. Scale bar (Day 13 image) represents 1500 µm.

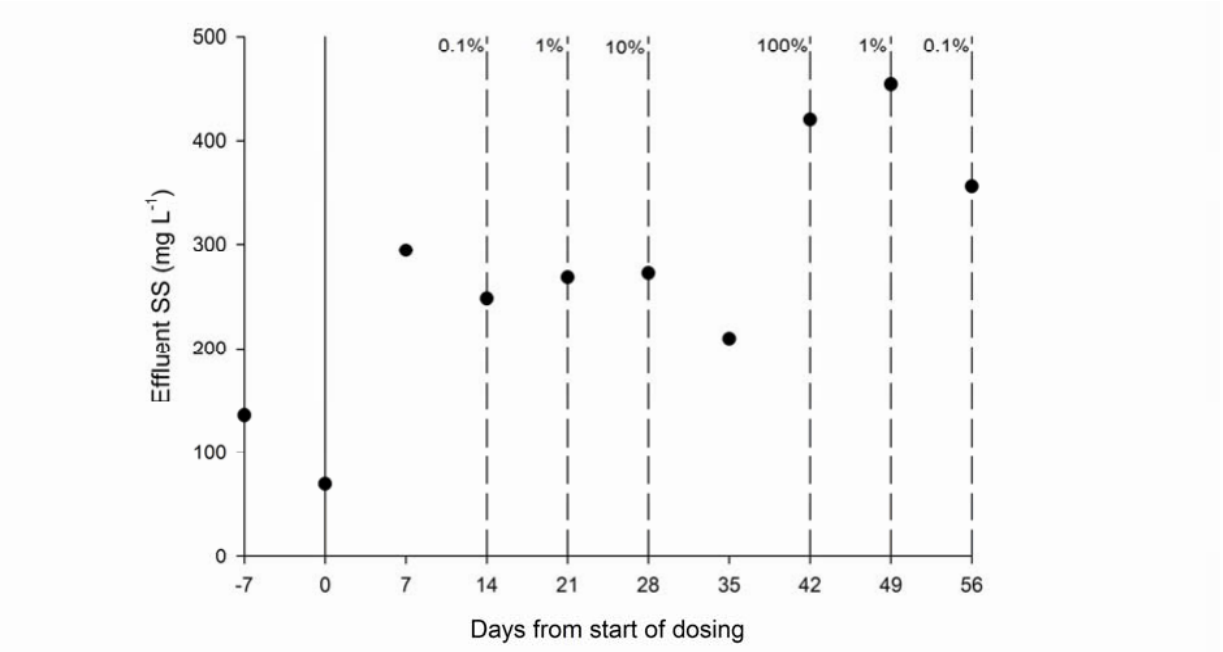

Figure S6. Effluent suspended solids (SS). Dotted lines represent the ends of a particular dosing regime and indicate the OC dosing level as a percentage of the maximum dose.

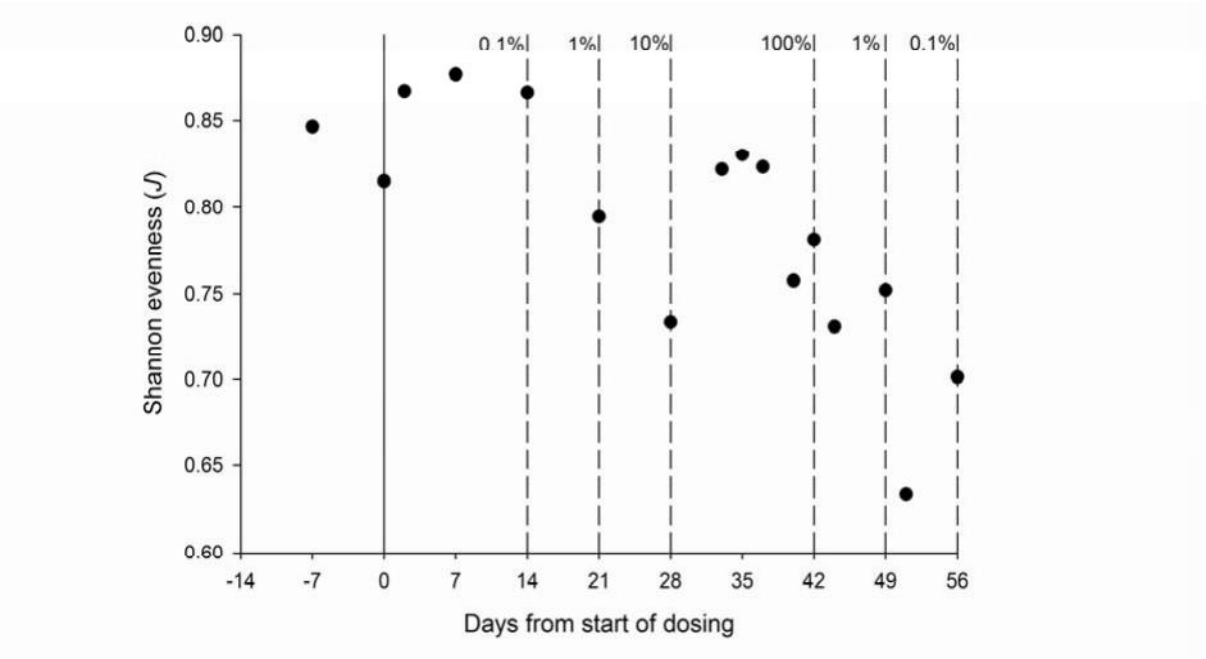

Figure S7. Shannon evenness (*J*) derived from T-RFLP data. Dotted lines represent the ends of a particular dosing regime and indicate the OC dosing level as a percentage of the maximum dose.

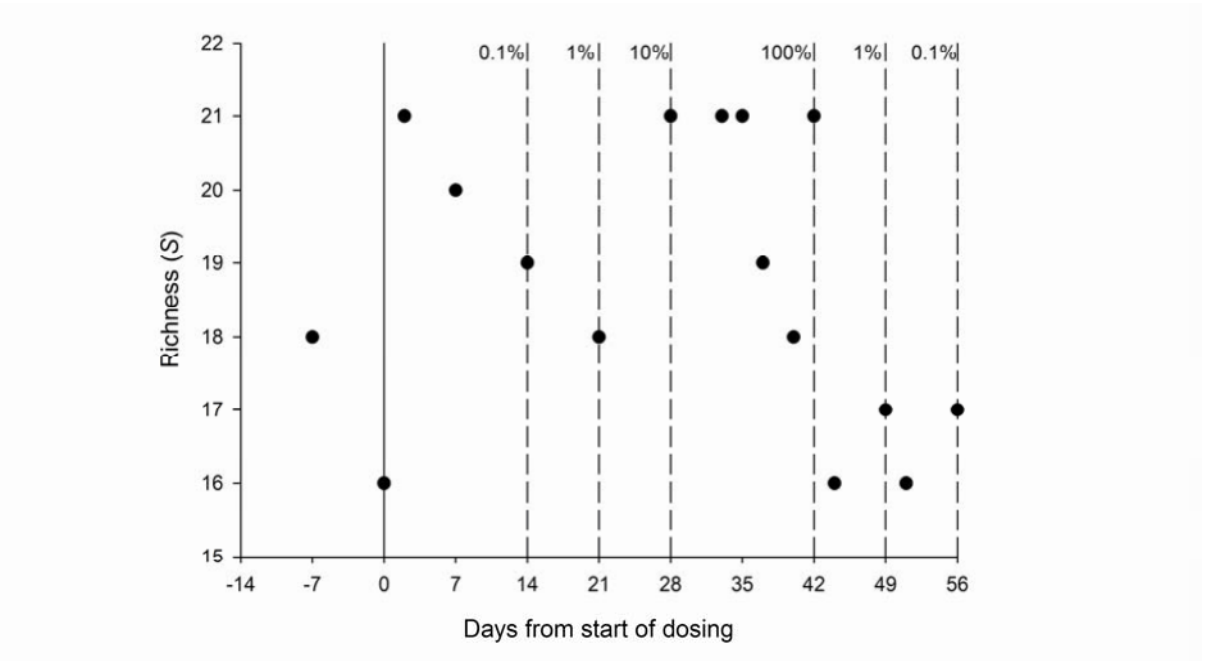

Figure S8. Richness (*S*) derived from T-RFLP data. Dotted lines represent the ends of a particular dosing regime and indicate the OC dosing level as a percentage of the maximum dose.

References

Crocetti, G.R., Hugenholtz, P., Bond, P.L., Schuler, A., Keller, J., Jenkins, D. and Blackall, L.L. (2000) Identification of polyphosphate-accumulating organisms and design of 16S rRNA-directed probes for their detection and quantitation. Applied and Environmental Microbiology 66(3), 1175-1182. Crocetti, G.R., Banfield, J.F., Keller, J., Bond, P.L. and Blackall, L.L. (2002) Glycogen-accumulating organisms in laboratory-scale and full-scale wastewater treatment processes. Microbiology-Sgm 148, 3353-3364.

Daims, H., Bruhl, A., Amann, R., Schleifer, K.H. and Wagner, M. (1999) The domain-specific probe EUB338 is insufficient for the detection of all Bacteria: Development and evaluation of a more comprehensive probe set. Systematic and Applied Microbiology 22(3), 434-444.

Daims, H., Lucker, S. and Wagner, M. (2006) *daime*, a novel image analysis program for microbial ecology and biofilm research. Environmental Microbiology 8(2), 200-213.

Kong, Y.H., Ong, S.L., Ng, W.J. and Liu, W.T. (2002) Diversity and distribution of a deeply branched novel proteobacterial group found in anaerobic-aerobic activated sludge processes. Environmental Microbiology 4(11), 753-757.

Marchesi, J.R., Sato, T., Weightman, A.J., Martin, T.A., Fry, J.C., Hiom, S.J. and Wade, W.G. (1998) Design and evaluation of useful bacterium-specific PCR primers that amplify genes coding for bacterial 16S rRNA. Applied and Environmental Microbiology 64(2), 795-799.

Slater, F.R., Johnson, C.R., Blackall, L.L., Beiko, R.G. and Bond, P.L. (2010) Monitoring associations between clade-level variation, overall community structure and ecosystem function in enhanced biological phosphorus removal (EBPR) systems using terminal-restriction fragment length polymorphism (T-RFLP). Water Research 44(17), 4908-4923.

Smolders, G.J.F., Vandermeij, J., Vanloosdrecht, M.C.M. and Heijnen, J.J. (1994) Model of the anaerobic metabolism of the biological phosphorus removal process - stoichiometry and pH influence. Biotechnology and Bioengineering 43(6), 461-470.